agronomy

MDPI

Article

Effects of Straw Return on Soil Physicochemical Properties and Microbial Communities in a Cold-Region Alkaline Farmland

Wei Zhang [1], Jinghong Wang [1], Aman Khan [2], Guinan Shen [3], Dan Wei [4,*] and Weidong Wang [1,2,*]

[1] Key Laboratory of Low-Carbon Green Agriculture in Northeastern China, Ministry of Agriculture and Rural Affairs, College of Agriculture, Heilongjiang Bayi Agricultural University, Daqing 163000, China
[2] Key Laboratory of Saline-Alkali Vegetation Ecology Restoration, Ministry of Education, College of Life Sciences, Northeast Forestry University, Harbin 150040, China
[3] Key Laboratory of Low-Carbon Green Agriculture in Northeastern China, Ministry of Agriculture and Rural Affairs, College of Life Science and Biotechnology, Heilongjiang Bayi Agricultural University, Daqing 163000, China
[4] Institute of Plant Nutrition and Resources, Beijing Academy of Agricultural and Forestry Sciences, Beijing 100081, China
* Correspondence: wd2087@163.com (D.W.); wdwang@nefu.edu.cn (W.W.)

Abstract

Straw return is crucial for sustainable agriculture, but its efficiency is limited by low temperatures in cold regions, especially in saline-alkali soils. This study investigates the degradation process of maize straw and the response of soil properties and microbial communities during the winter low-temperature period in the alkaline farmland of Anda, China. A two-year field experiment with straw return (SR) and no return (NR) treatments was conducted. Straw degradation rates and structural changes (as observed via scanning electron microscope, SEM) were monitored. Soil physicochemical properties and enzyme activities were analyzed. Microbial community composition was characterized using 16S rRNA and ITS sequencing. The cumulative straw degradation rate over two years reached 94.81%, with 18.33% occurring in the first winter freeze–thaw period. Freeze–thaw cycles significantly damaged the straw structure, facilitating microbial colonization. Straw return significantly improved soil properties after winter, increasing field water capacity (3.45%), content of large aggregates (6.57%), available nutrients (P 38.17 mg/kg, K 191.93 mg/kg), and organic carbon fractions compared to NR. Microbial analysis revealed that low temperatures filtered the community, enriching cold-tolerant taxa like *Pseudogymnoascus*, *Penicillium*, and *Pedobacter*, which are crucial for lignocellulose decomposition under cold conditions. The winter period plays a significant role in initiating straw degradation in cold regions. Straw return mitigates the adverse effects of winter freezing on soil quality and promotes the development of a cold-adapted microbial consortium, thereby enhancing the sustainability of alkaline farmland ecosystems in Northeast China.

Keywords: freeze–thaw cycles; straw decomposition; saline-alkali soil; soil nutrients; soil microbial diversity

check for updates

Academic Editor: Witold Grzebisz

Received: 19 September 2025
Revised: 14 October 2025
Accepted: 16 October 2025
Published: 21 October 2025

Citation: Zhang, W.; Wang, J.; Khan, A.; Shen, G.; Wei, D.; Wang, W. Effects of Straw Return on Soil Physicochemical Properties and Microbial Communities in a Cold-Region Alkaline Farmland. *Agronomy* **2025**, *15*, 2433. https://doi.org/10.3390/agronomy15102433

Copyright: © 2025 by the authors. Licensee MDPI, Basel, Switzerland. This article is an open access article distributed under the terms and conditions of the Creative Commons Attribution (CC BY) license (https://creativecommons.org/licenses/by/4.0/).

1. Introduction

Returning straw to the soil is an effective practice for enhancing the sustainable use of arable land, helping to mitigate the progressive decline in soil quality associated with continuous agricultural exploitation [1]. The degradation of returned straw plays a critical role in nutrient cycling, maintaining soil health, and contributing to soil carbon stocks [2].

Straw decomposition in the soil is primarily influenced by environmental factors [3], soil type [4,5], straw types [6,7], microbial community structure [8], and cultivation practices [9]. Among these, seasonal temperature fluctuations exert a significant and predictable influence on straw decomposition dynamics and soil microbial activity [10]. In the seasonal temperature fluctuation, the prolonged low winter temperatures in cold regions significantly inhibit both straw degradation and soil microbial activity. Studies have shown that straw decomposition rates are higher in warmer seasons compared to colder ones [9,11,12], and higher in temperate zones than in frigid zones. For example, a two-year field study on straw degradation across Hailun, Fengqiu, and Yingtan in China found that the degradation rate at the Hailun site, located in the cold-temperate zone, was markedly lower than at Fengqiu and Yingtan, which are situated in warmer climatic zones [13].

Straw return to the field generally occurs after the autumn harvest, where mechanically crushed straw is buried or left on the soil surface. Under the influence of seasonal climate fluctuations, ultraviolet radiation, and microbial succession, the straw gradually breaks down into soluble sugars, organic acids, nitrogen, and other nutrients. This process not only enriches the soil but also stimulates the mineralization of native organic matter and promotes the formation of soil aggregates, enhancing soil carbon stability [14,15]. Common microorganisms involved in straw degradation include Penicillium, Trichoderma, Chloroflexi, Ascomycota, and Basidiomycota, among others [1,8,10,12]. In cold regions, temperatures drop rapidly after the autumn harvest, leading to repeated freeze–thaw cycles. These cycles cause the formation and recrystallization of irregular ice crystals in the soil and straw, which physically damage straw tissues, reduce mass, and increase surface area exposure. Continued freezing can also lead to soil water loss and protein denaturation, further affecting decomposition processes [16,17]. The decomposition of organic matter in nature depends primarily on fungi and bacteria [18]. The increased surface area of straw following freeze–thaw events provides better microbial attachment sites, enhancing decomposition potential. However, temperature is a key driver of microbial community structure [19,20], and prolonged cold weakens most microorganisms [21]. This results in slower straw degradation, increased residue accumulation, and potential competition between microbes and crops for nutrients during the following spring, which may negatively impact crop yield [22]. Tsegaye [23] reported that in the southeastern United States, where winter temperatures below 0 °C typically last only 10–20 days, the carbon sequestration of soils with straw cover during winter could offset the carbon losses from soil respiration in summer. In contrast, Northeast China, home to the world's third-largest black soil region, experiences long, harsh winters. In Heilongjiang Province, situated in the cold-temperate zone of the Northern Hemisphere, temperatures drop rapidly following the fall harvest (October), and remain low until the pre-sowing period in April. During this time, soils undergo extended freezing for approximately 137–176 days, with 22–46 freeze–thaw cycles occurring in spring (data sourced from the National Weather Information Center, http://data.cma.cn/, accessed on 10 July 2025) [24,25]. These seasonal low temperatures significantly hinder the degradation of returned straw, which typically reaches only 50–70% [26], and also suppress the activity of soil microorganisms, the primary agents driving straw decomposition. In China, the area of saline-alkali farmland is approximately 11.5 million hectares, with the Northeast accounting for about 26% [27]. As temperatures decrease and the soil freezes, salt migration is primarily driven by water transport, influenced by temperature gradients. Salts accumulate at the freezing front and eventually concentrate in the surface layer, with local salt concentrations potentially reaching three times the initial value [28,29]. Fluctuations in soil salinity do not alter the core composition of microbial communities, but significantly alter the relative abundance of dominant species, increasing the difficulty of straw decomposition during the low-temperature period [30]. The extreme environmental shifts can reduce microbial diversity, leading to convergence in microbial

communities across regions [31]. This suggests that cold-tolerant microorganisms contributing to straw decomposition in winter can be identified by analyzing community shifts in cold and saline agricultural soils. Current research on cold-adapted microorganisms has largely focused on extreme environments such as the Arctic [32] and glaciers [33], or industrial applications like low-temperature pulping [34] and low-temperature washing [35]. However, relatively little attention has been paid to microbial community dynamics in farmland soils during winter in cold and saline agricultural regions, highlighting a gap in understanding microbial contributions to straw degradation under field conditions. This study aimed to do the following: (i) quantify the structural degradation of returned maize straw during the winter low-temperature period; (ii) assess the concomitant changes in soil physicochemical properties; and (iii) identify the key cold-tolerant microorganisms responsible for straw degradation in the saline-alkali soil of Northeast China.

2. Materials and Methods

2.1. Experimental Site

The field experiment sites were set up from October 2021 to October 2023 at the Anda Experimental Base of Heilongjiang Bayi Agricultural University in Anda City, Heilongjiang Province, China (46.41° N, 125.36° E). The soil type in this area is calcareous black and saline (pH 8.0–9.0, total salt content 0.13–0.22%, data referenced to Soil Science Database http://vdb3.soil.csdb.cn/, accessed on 12 July 2025), with a cold and dry winter lasting over 200 days, an average sunshine duration of 2659 h, an annual average temperature of 3.2 °C, and a frost-free period of 136 days. It belongs to the northern temperate continental semi-arid monsoon climate. According to 30 consecutive years of data from the China Meteorological Administration, the average monthly maximum temperature in March, April, October, and November, when freezing and thawing occur, is 13.6 °C, and the minimum temperature is −10.9 °C (data referenced to National Weather Information Center http://data.cma.cn/, accessed on 10 July 2025). The temperature difference is about 20 degrees. The experiment selected two adjacent soil plots measuring 5 m × 30 m each, applying straw return and non-return treatments. Each experimental plot measures 50 m^2, with three replicates per treatment.

2.2. Field Straw Decomposition Experiment

According to the experimental requirements, two treatments were set up in the experimental field at the Anda Experimental Base of Heilongjiang Bayi Agricultural Reclamation University: straw return treatment (SR) and non-straw return (NR) treatment. For the straw return treatment plots, after the fall harvest, the stalks were cut into small sections of 1–3 cm in length and returned to the field, and the amount of return was calculated according to the annual yield of the stalks, i.e., 7538.1 kg ha^{-1}, at a depth of 20 cm. At the same time, 72 nylon bags containing 10 g of straw were buried in the straw return field, and samples were taken regularly (3 replications) to determine the straw degradation rate. The low-temperature period was from October to April of the following year, covering the low-temperature freeze–thaw period in autumn, the long freeze period in winter, and the low-temperature freeze–thaw period in spring. Sampling times are divided into before and after the low-temperature period based on temperature fluctuations (BL and AL). Three treatment groups were formed based on different management practices: BLNR (before low-temperature period (BL) with no residue incorporation (NR)), ALNR (after low-temperature period (AL) with no residue incorporation (NR)), and ALSR (after low-temperature period (AL) with residue incorporation (SR)).

2.3. Indoor Low-Temperature Period Simulation Experiment

The soil for the simulation test was taken from the agronomy experimental field on the campus of Heilongjiang Bayi Agricultural University, and the soil was sieved through a 5 mm sieve, mixed well, and sterilized; then, 1.3 kg of soil was packed into a cylindrical plastic box of 16 cm height and 16 cm diameter, and the moisture content was adjusted to 15%, and then left to stand for 30 days. The crushed 1–3 cm long corn stover segments of 15 g were packed into a nylon bag (triplicate) and placed 8 cm below the soil to simulate the burial of stover in the field. At 19:00 h every day, the soil was placed in the refrigerator at −15 °C to simulate freezing conditions, and at 9:00 h, it was taken out and placed in the environment at 10 °C to simulate thawing conditions, simulating the freezing and thawing phenomena in autumn and spring. Separate simulations were conducted for 20, 35, 50, 65, 80, and 95 freeze–thaw cycles; after 50 freeze–thaw cycles, some samples (triplicate) were subjected to prolonged freezing in a −15 °C freezer to create an indoor simulation test for cold-region winter climate conditions—incorporating autumn freeze–thaw cycles, prolonged low-temperature freezing in winter, and spring freeze–thaw cycles—and to investigate the effects of different freeze and thawing times on the structure of the stalks, to determine the main period of straw decomposition during the low-temperature period.

2.4. Straw Sample Collection and Determination

Straw samples were processed through shredding, with original samples retained for comparison. Sampling for straw degradation testing was conducted in April, May, June, July, August, September, and October of both 2022 and 2023. Nylon bags (3 replications) buried in plastic boxes and soil were removed and cleaned with water. Some of the samples were washed and air-dried for scanning electron microscopy analysis, and some of the samples were dried and pulverized for measurement. The rate of straw degradation was calculated using the weight loss method, and cellulose, hemicellulose, and lignin were measured by a VELP-FIWE semi-braked cellulose tester (FIWE3/6, VELP, Usmate, Italia).

2.5. Soil Sample Collection and Determination

Soil samples were collected in October 2022 from plots where straw was not returned to the field and from plots where straw was returned to the field, and in April 2023 from plots where straw was returned to the field. A 500 g sample of soil at the field trial site was taken at 0–20 cm by a five-point sampling method with three replicates for each subgroup, stored on ice, and transported to the laboratory. Part of each sample was stored in a −80 °C refrigerator for microbial high-throughput sequencing, part of the sample was air-dried, and part of the sample was stored in a −20 °C refrigerator for soil physicochemical property analysis. Sampling times were October after the fall harvest and April after the end of the spring freeze–thaw.

During soil sampling, additional soil collection boxes and ring knives were utilized to collect 500 g of intact soil clods 0–20 cm deep without destroying the soil structure for soil physical property analysis. Soil bulk density and field water-holding capacity were determined by the ring knife method; water-stable aggregates were determined by the wet sieve method [36,37].

Total nitrogen was determined by the semi-micro Kjeldahl method; total phosphorus was determined by the sulfuric acid–perchloric acid method; ammonium nitrogen was determined by the KCl leaching-indigo phenol blue colorimetric method; nitrate nitrogen was determined by the dual-wavelength ultraviolet spectrophotometric method; available phosphorus was determined by the sodium bicarbonate leaching-molybdenum antimony colorimetric method; available potassium was determined by the ammonium acetate leaching-flame photometry method; pH was determined by the potentiostatic meter method (water-soil ratio of 2.5:1);

the organic matter was determined by high-temperature exothermic potassium dichromate oxidation-volumetric method [38]. The total carbon, total organic, recombinant organic carbon, water-soluble organic carbon, readily oxidizable organic carbon, and microbial carbon (direct extraction by chloroform fumigation) were determined using the Elementar Vario EL Cube elemental analyzer (Elementar, FrankfurtRhineMain, Germany) and Shimadzu TOC-LCPH organic carbon analyzer (Shimadzu, Tokyo, Japan).

Enzyme activity for cellulose and hemicellulose degradation (Exo-β-1,4-glucosidase, Endo-β-1,4-glucanase, Glucosidase, filter paper activity and Xylanase, Mannanase, Galactosidase, Arabinosidase) were determined using the DNS method; enzyme activity for ligninase degradation (Lignin peroxidase, manganese peroxidase and laccase) was determined using the veratryl alcohol method for lignin peroxidase, the $MnSO_4$ method for manganese peroxidase, and the ABTS method for laccase [39,40].

2.6. Microbial High-Throughput Sequencing

Total DNA was extracted from soil samples using a soil DNA extraction kit (M5635-02, OMEGA Bio-Tek, Norcross, GA, USA). These DNA samples were sent to Shanghai Personal Biotechnology Co., Ltd., (Shanghai, China) where 16S rRNA and ITS amplicon sequencing of DNA fragments was performed using the Illumina NovaSeq 6000 Sequencer (NovaSeq 6000, Illumina, San Diego, CA, USA). Sequence denoising, sequence length distribution, classification, and phylogenetic tree construction were performed using QIIME2 (2022.11) and custom scripts. The resulting ASV data were analyzed on the cloud platform of Shanghai Personal Biotechnology Co., Ltd. (https://www.genescloud.cn, accessed on 1 July 2025).

2.7. Data Analysis

SPSS 18.0 statistical analysis software was used for mean comparison, F-tests to assess the homogeneity of variances among sample groups, and *t*-tests to analyze mean differences between samples (significance level set at $p = 0.05$). Graphs were generated using Origin 2021.

3. Results and Discussion

3.1. Effects of the Low-Temperature Period on the Straw Structure

Field observations of straw degradation showed the degradation rate of returned straw over two consecutive years. In the first year, 77.16% of the straw degraded, while only 17.65% of straw was degraded in the second year, resulting in a cumulative degradation rate of 94.81% over the two years (Figure 1A). For the primary components of straw, cellulose degradation reached 80.61% in the first year and 15.7% in the second year. Hemicellulose degradation was 80.81% in the first year, followed by 15% in the second year. Lignin degradation was lower, at 56.03% in the first year and 35.31% in the second year. Over the two years, total degradation was 96.31% for cellulose, 96.84% for hemicellulose, and 85.34% for lignin. During the first freezing period, 18.33% of the straw decomposed, accounting for about 23.76% of total straw degradation in the first year. During this period, cellulose, hemicellulose, and lignin degraded by 16.96%, 23.58%, and 20.79%, respectively. These amounts represented 20.99%, 29.18%, and 37.11% of the total annual degradation for these components in the first year. As shown in Figure 1B, SEM revealed that surface grooves and cracks on the straw became more prominent after the freezing period. Cross-sectional analysis revealed that each freeze–thaw cycle progressively degraded the straw structure. The first cycle caused breakage and filamentation, while the second cycle produced visible perforations.

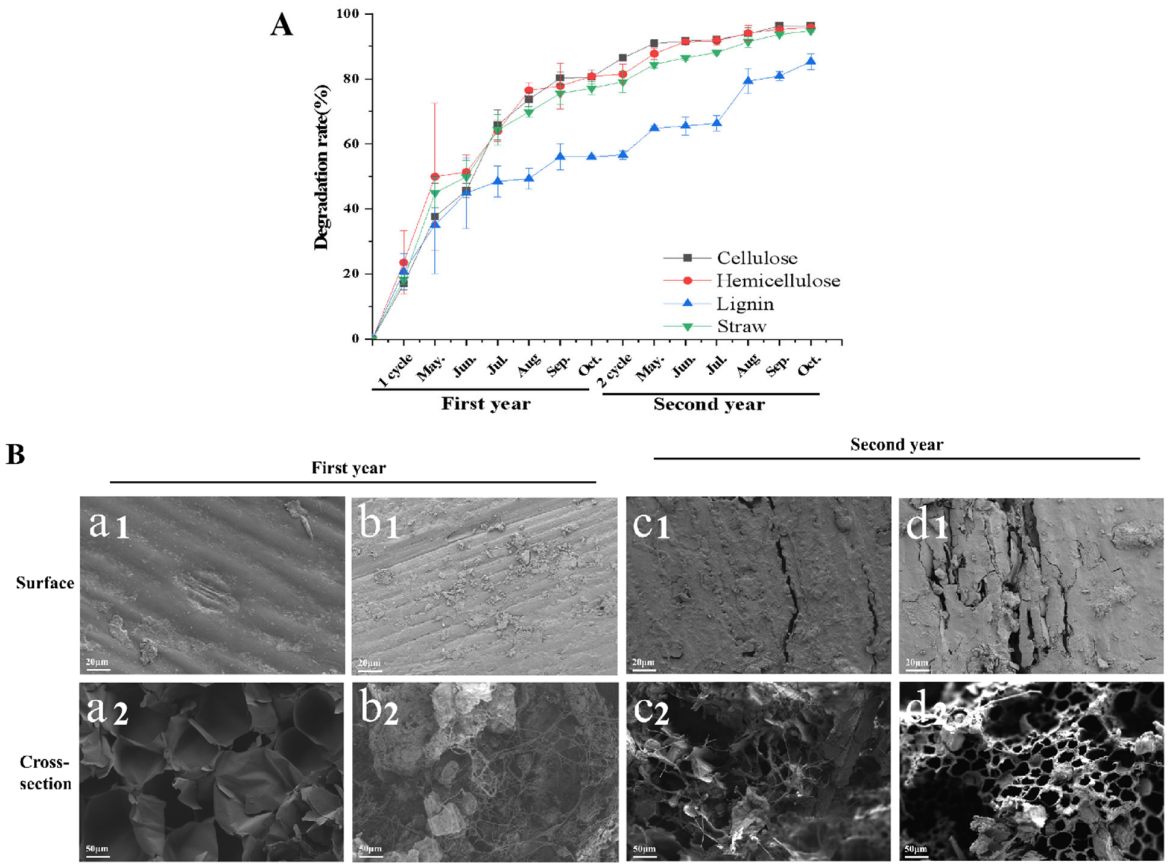

Figure 1. Degradation of returned straw (**A**) and SEM before and after freezing and thawing (**B**) (cycle: October–April of the following year; (**a1**): Suface–original straw; (**b1**): Suface–after the first low-temperature period; (**c1**): Suface–after 1 year of degradation; (**d1**): Suface–after the second low-temperature period; (**a2**): Cross–section–original straw; (**b2**): Cross–section–after the first low-temperature period; (**c2**): Cross–section–after 1 year of degradation; (**d2**): Cross–section–after the second low-temperature period).

In the North China Plain, the annual decomposition rate of straw returned to the field is approximately 65% [41]. This finding is consistent with the results of this study, which observed a one-year degradation rate of about 70%. Furthermore, it was quantified that the initial low-temperature period alone accounted for roughly one-quarter of the first year's total decomposition (Figure 1A). While existing research on freeze–thaw cycles has predominantly focused on their erosive effects on resilient materials like rock, soil, and concrete [42–44], this study demonstrates that the same principle applies to straw. Given its less resilient texture, straw is subject to even more rapid and pronounced physical degradation. This assertion is directly supported by electron microscopy images, which reveal significant structural erosion of straw following in-field freeze–thaw cycles (Figure 1B).

SEM analysis of the simulated experiments showed the effect of different freeze–thaw cycles on the organization and structure of corn stover (Figure 2). The surface morphological changes became evident after approximately 50 freeze–thaw cycles, which appeared to mark a critical threshold. Initially, with increasing cycles, the surface veins of the straw smoothed out; however, as the cycles progressed, these veins deepened, and visible surface cracking emerged after 80 cycles. In terms of cross-sectional structure, the straw initially displayed regularly arranged, fan blade-like pores. With continued freeze–thaw exposure, these structures gradually deformed, folding and eventually fracturing. Notably, after approximately 65 cycles, prominent holes began to appear on the cross-sectional surface, indicating progressive structural degradation. These observations suggest that repeated

freeze–thaw cycles significantly compromise the integrity of corn stover, both at the surface and internal levels. Successive cryogenic freezing without thawing did not change the surface or cross-sectional structure of the straw.

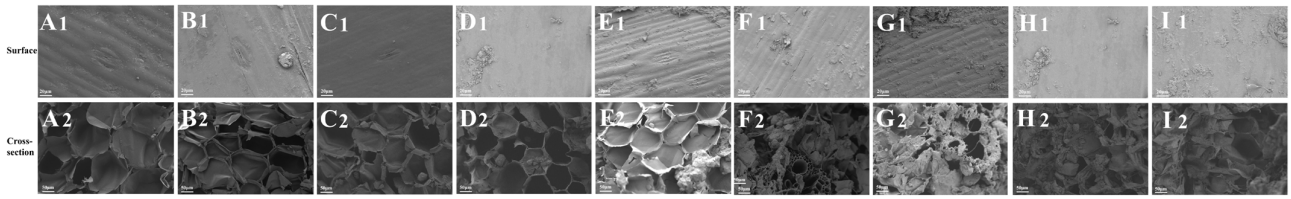

Figure 2. SEM image of indoor freeze–thaw simulation test ((**A**): original straw; (**B**): 20 times freezing and thawing; (**C**): 35 times freezing and thawing; (**D**): 50 times freezing and thawing; (**E**): 65 times freezing and thawing; (**F**): 80 times freezing and thawing; (**G**): 95 times freezing and thawing: before long freezing period; (**H**): before long freezing period; (**I**): after long freezing period; Number 1: Suface; Number 2: Cross–section).

The low-temperature period in this region extends from October to the following April. This duration encompasses the autumn freeze–thaw period, the sustained frozen period in winter, and the spring freeze–thaw period. The mechanism by which freeze–thaw cycles accelerate material degradation involves three primary factors: (1) repeated temperature fluctuations, (2) the phase change in water between solid and liquid states within the material, and (3) the frequency and total number of cycles [45,46]. Some studies have shown that the larger the number of freeze–thaw cycles, the larger the range of temperature fluctuations and the faster the frequency; the more destructive the process is to the material; and the larger the water content of the material and the pores formed during the solid–liquid conversion of moisture [44]. Conversely, the intrinsic properties of a material determine its resistance to this damage. Materials with lower inherent porosity, lower permeability, and higher mechanical strength generally demonstrate greater resilience to the destructive forces of freeze–thaw cycles [42]. Experimental results confirm that while low-temperature freezing alone caused no visible structural damage to the straw, progressive degradation occurred with increasing freeze–thaw cycles. SEM revealed increasingly apparent surface destruction and significantly more structural disruption in porous cross-sections compared to intact surfaces (Figure 2). The findings demonstrate that in cold regions during low-temperature periods, straw degradation occurs primarily during the autumn and spring freeze–thaw periods rather than the sustained winter freeze (Figures 1 and 2).

3.2. Physicochemical Characteristics and Microbial Diversity of Saline Soil

After prolonged exposure to low-temperature conditions, the soil bulk density and porosity showed no significant changes before and after the low-temperature period (Figure 3A). The field water-holding capacity of the ALNR group (21.83%) was significantly lower compared to the BLNR group (23.20%) (Figure 3B). As shown in Figure 3C, the BLNR treatment groups had a significantly higher proportion of water-stable aggregates in the 5–0.5 mm size range compared to the ALNR group. The content of large aggregates (>0.25 mm) was notably higher in the BLNR (86.64%) treatments than in the ALNR group. The BLNR had significantly higher levels of soil available nutrients, except for nitrate nitrogen, compared to the ALNR groups. The results revealed that ammonium nitrogen, available phosphorus, and available potassium in the BLNR group were 12.92 mg/kg, 28.63 mg/kg, and 124.93 mg/kg; nitrate nitrogen content showed no significant differences between groups (Figure 3D). In terms of soil salinity, soil pH significantly decreased after the low-temperature period; total salt content did not differ significantly (Figure 3E). In terms of carbon content in soil, the BLNR group also showed lower levels of total carbon (25.20 g/kg), reconstituted organic carbon (7.59 g/kg), and readily

oxidizable organic carbon (1.65 g/kg), in comparison to the ALNR group; the total organic carbon, water-soluble organic carbon, and microbial carbon were not significant differences between the two groups (Figure 3F). The enzyme activity for cellulose and hemicellulose degradation (Exo-β-1,4-glucosidase, Endo-β-1,4-glucanase, Glucosidase, Filter paper activity and Xylanase, Mannanase, Galactosidase, Arabinosidase) showed that BLNR was significantly higher than ALNR (Figure 3G,H) while the enzyme activity for ligninase degradation (Lignin peroxidase, manganese peroxidase and laccase) in the two groups was low (Figure 3I).

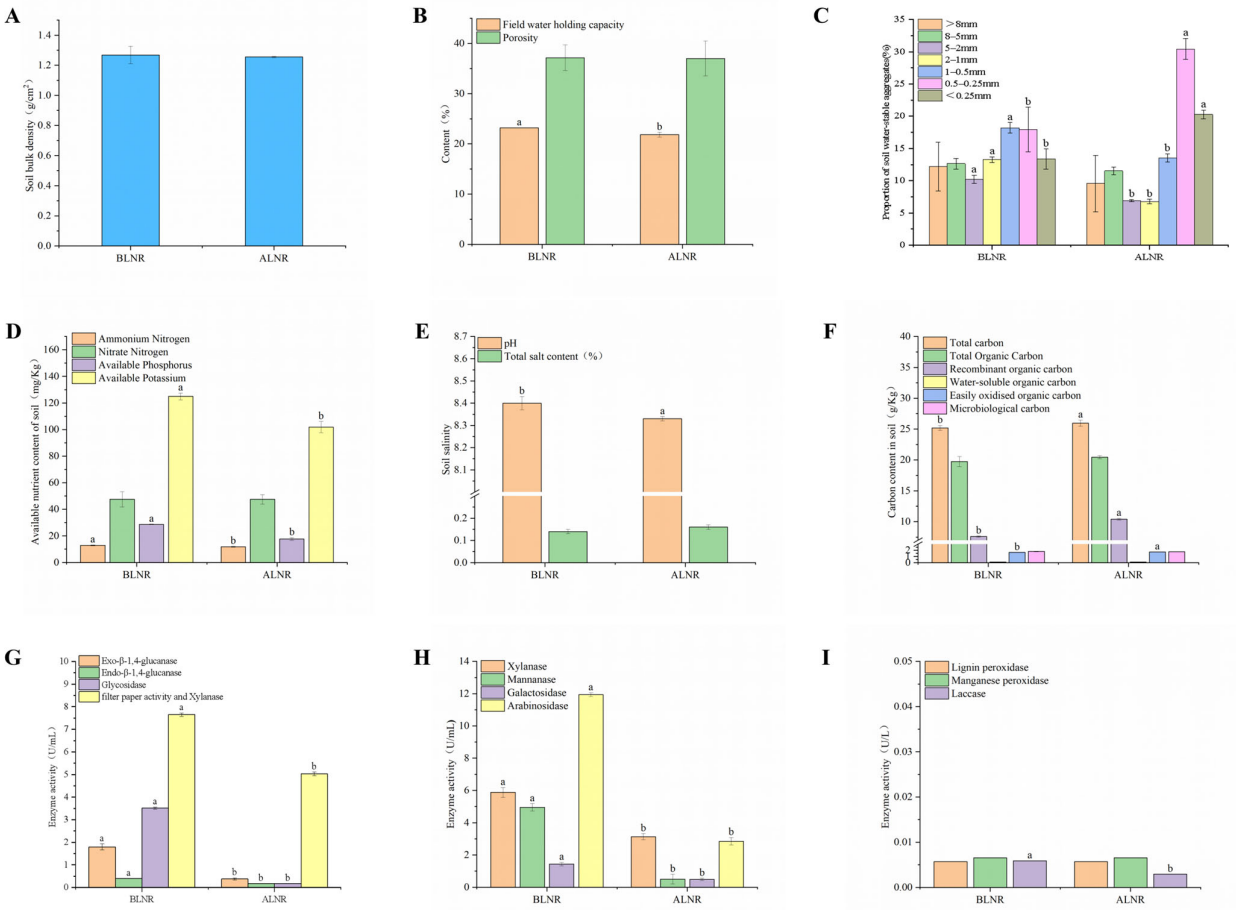

Figure 3. Effects of the low-temperature period on soil physical and chemical properties and enzyme activity (**A**): soil bulk weight; (**B**): soil field water-holding capacity and soil porosity; (**C**): soil water-stable aggregates; (**D**): soil available nutrients; (**E**): soil salinity; (**F**): carbon content in soil; (**G**): enzyme activity for cellulose degradation; (**H**): enzyme activity for hemicellulose degradation; (**I**): enzyme activity for lignin degradation). Clearly labeled is the significance level ($p < 0.05$) indicated by different lowercase letters (a, b) within each subplot (A, B, C, etc.).

It has been reported that the bulk density of farmland soil transitions from a relatively stable state during the early low-temperature period to a rapid decline during the freezing period, followed by relative stability until the thawing period begins. The repeated freeze and thaw cycles typically cause a gradual increase in soil bulk density before it stabilizes [47,48]. However, this experiment observed no significant difference in soil bulk density values before and after the low-temperature period (Figure 3A). This divergence from established trends may be attributed to a self-repair mechanism within the soil. Studies on black soil have demonstrated that freeze–thaw cycles increase total porosity. However, this often involves a shift towards more slender, ineffective pores, which subsequently reduces the soil's field water capacity, showing a negative correlation [49]. The results of this study align with this principle; while no significant change in total porosity was detected, a significant reduction

in field water-holding capacity was observed after freeze–thaw cycles (Figure 3B). With the constant fluctuation of temperature during the cold period, the process of freezing to form ice crystals and thawing is constantly repeated by the moisture in the soil inside the agglomerates, and the expansion of the volume during the formation of ice crystals can easily lead to the fragmentation of large aggregates and their decomposition into small aggregates or even dispersed soil particles [50,51]. However, Zhang found that fall freeze–thaw cycles increased the content of aggregates with 2–5 mm and 0.25–2 mm grain sizes in soils, and the proportion of large aggregates broken down increased under the influence of spring freeze–thaw [52]. The results of this experiment only observed that the composition of macroaggregate in the soil was lower after the soil freeze–thaw period than before the freeze–thaw (Figure 3C). Repeated freezing and thawing can cause drastic changes in soil moisture, which can easily lead to a leaching phenomenon resulting in soil nutrient loss [53]. In terms of fast-acting nutrients, only nitrate nitrogen showed no difference before and after the low-temperature period, while all others were significantly lower than before the low-temperature period (Figure 3D). As temperatures decrease and the soil freezes, salt migration is primarily driven by water transport, influenced by temperature gradients. Salts accumulate at the freezing front and eventually concentrate in the surface layer, with local salt concentrations potentially reaching three times the initial value [28,29]. The results of this experiment were different from those reported previously. There was no difference in the total salt content of the soil, but the pH decreased significantly (Figure 3E). It was found that freeze–thaw cycles accelerate the decomposition and migration of organic carbon through three mechanisms: physical fragmentation, chemical dissolution, and microbial activation, especially in cold and humid regions [54]. In terms of carbon pools, differences in total organic carbon, restructured organic carbon, and easily oxidizable carbon were observed before and after the low-temperature period (Figure 3F). The addition of exogenous nutrients in the right environment, such as temperature, moisture content, etc., can effectively promote the production of enzymes by soil microorganisms [10,55]. In this paper, enzyme activity presented by BLNR is better than that of ALNR (Figure 3G,H). Microbial biomass carbon (MBC), an important indirect response to the amount and activity of microorganisms in the soil, is positively correlated with the soil C cycle [56], with microbial residues accounting for 60% of the total carbon in the soil [57]. The microbial carbon in the BLNR group, indicating that the microorganisms in the soil could be MBC, an important indirect response to the amount and activity of microorganisms in the soil, is positively correlated with the soil C cycle, with microbial residues accounting for 60% of the total carbon in the soil. Filter paper enzyme, xylanase, mannanase, and arabinogalactanase were more active than those related to the difficult-to-decompose lignin (Figure 3E,G–I).

The soil bulk density of the ALSR group was 1.07 g/cm^3, which was significantly lower than in the ALNR (1.26 g/cm^3) treatments (Figure 4A). ALSR treatment exhibited a field water-holding capacity of 25.27% and soil porosity was 49.13%, significantly greater than those observed in the ALNR group (Figure 4B). As shown in Figure 4C, the ALSR treatment group had a significantly higher proportion of water-stable aggregates in the 5–0.5 mm size range compared to the ALNR group. The content of large aggregates (>0.25 mm) was also notably higher in the ALSR treatments than in the ALNR group. The ALSR treatment had significantly higher levels of soil available nutrients, except for nitrate nitrogen, compared to the ALNR group. The results revealed that ammonium nitrogen, available phosphorus, and available potassium in the ALSR group were 14.99 mg/kg, 38.17 mg/kg, and 191.93 mg/kg, respectively, while nitrate nitrogen was low at 24.15 mg/kg compared to ALNR (Figure 4D). As shown in Figure 4E, the pH value of the ALSR group was significantly lower than that of the ALNR group, at 8.26. There was no significant difference in total soil salt content, but the ALSR group had the lowest value, at 0.14. In terms of carbon content in soil, the ALSR group also showed the higher levels of total carbon (27.73 g/kg), total organic carbon

(21.47 g/kg), reconstituted organic carbon (11.92 g/kg), water-soluble organic carbon (0.16 g/kg), and readily oxidizable organic carbon (2.23 g/kg), in comparison to the ALNR group (Figure 4F). Microbial carbon was significantly higher in ALSR than in ALNR. Four cellulase activities showed that ALSR exhibited the highest cellulase activity compared to ALNR (Figure 4G). Among the enzyme activity for cellulose degradation, filter paper enzyme activity was the highest overall. Similarly, the ALSR group exhibited the highest xylanase activity, reaching a maximum of 8.27 U/mL, which was significantly greater than that of the ALNR group. Mannanase activity in the ALSR soil was 4.34 U/mL, significantly higher than in the ALNR group. Additionally, arabinogalactanase activity in the ALSR group was significantly higher than in the ALNR group (Figure 4H). Very low enzyme activity for ligninase degradation (Lignin peroxidase, manganese peroxidase and laccase) in two groups (Figure 4I).

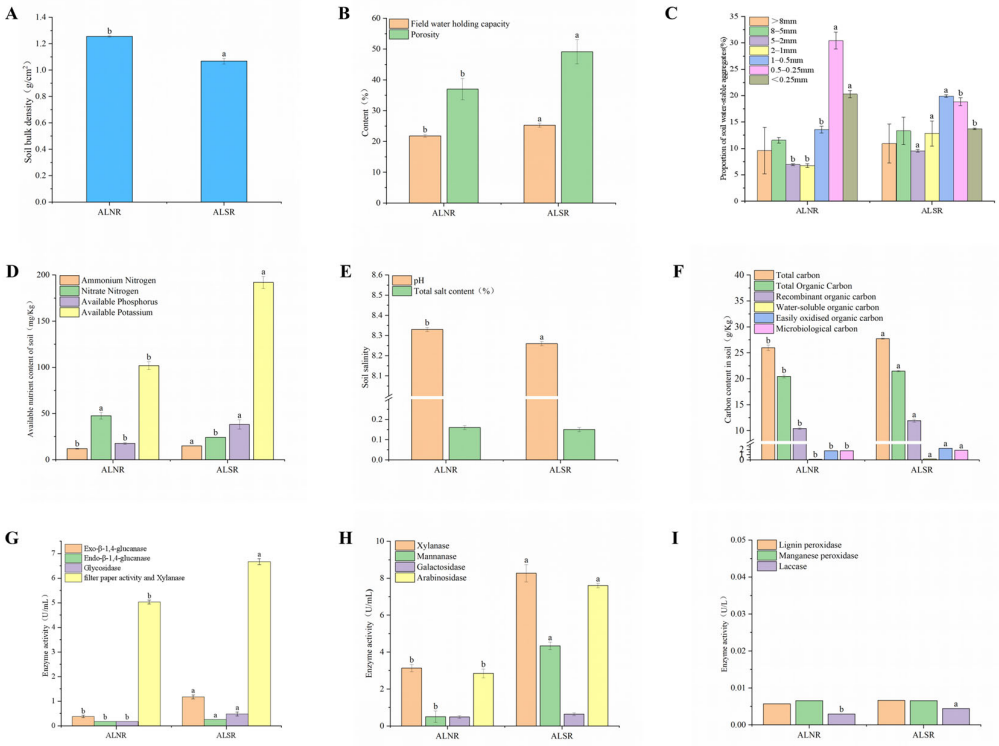

Figure 4. Effects of straw return to the field after a low-temperature period on soil physical and chemical properties and enzyme activity (**A**): soil bulk weight; (**B**): soil field water-holding capacity and soil porosity; (**C**): soil water-stable aggregates; (**D**): soil available nutrients; (**E**): soil salinity; (**F**): carbon content in soil; (**G**): enzyme activity for cellulose degradation; (**H**): enzyme activity for hemicellulose degradation; (**I**): enzyme activity for lignin degradation. Clearly labeled is the significance level ($p < 0.05$) indicated by different lowercase letters (a, b) within each subplot (A, B, C, etc.).

Straw return is a widely recognized practice for improving soil quality [58]. The method improves soil's thermal insulation properties and increases its resistance to freeze–thaw erosion. Furthermore, it reduces the evaporation of water in the soil, increases the water-holding capacity of the soil, and improves the physical structure of the soil [46]. The incorporation of straw effectively decreases the mass proportion of microaggregates while increasing the content of macroaggregates [59], thereby improving the stability of larger soil aggregates [60]. It was shown that different straw-returned treatments consistently reduce soil bulk density while increasing both field water-holding capacity and soil porosity. Specifically, straw application significantly preserved soil macroaggregate content, enhanced field water retention capacity, and reduced bulk

density (Figure 4A–C). With the decomposition of the returned straw, the nutrients in the straw were released into the soil, which effectively improved the nutrient content in the soil and increased the soil carbon storage [61]. The nutrient content of soil and soil C storage can be effectively maintained through straw return to the soil in this study (Figure 4D–F). Nutrients indirectly influence enzyme activity by regulating microbial biomass, residue decomposition rates, and microbial metabolic strategies. Studies have shown that appropriate nutrient levels and high-quality residue degradation can significantly enhance enzyme activity [62]. This is consistent with the results of this experiment, where straw gradually decomposes and releases nutrients after the low-temperature period, enhancing soil enzyme activity (Figure 4G–I). Returning crop residues to the field can effectively mitigate soil erosion during winter cold spells and improve soil physicochemical properties (Figures 3 and 4).

3.3. Microorganisms of Saline Soil

The changes before and after the low-temperature period are shown in Figure 5. At the fungi phylum level, a significant reduction in the dominant phylum Ascomycota was observed within BLNR (83.73%) compared to ALNR (90.51%) ($p < 0.05$). This represents a substantial decrease of 6.78% in BLNR relative to ALNR. Although not statistically significant, there was a decrease in Glomeromycota, as evidenced by large effect sizes ($p > 0.05$) (Figure 5A). In terms of bacteria, a total of twelve major phyla were detected: Acidobacteriota, Proteobacteria, Gemmatimonadota, Actinobacteriota, Chloroflexi, Methylomirabilota, Bacteroidota, Myxococcota, Planctomycetota, Nitrospirota, Latescibacterota, and Verrucomicrobiota. Analysis revealed that Proteobacteria and Verrucomicrobiota were significantly higher in the BLNR group compared to ALNR. There were other non-differentiating factors (Figure 5B). In the archaea domain, there were four main microbial groups: Crenarchaeota, Thermoplasmatota, Halobacterota, and Aenigmarchaeota. The results showed that Crenarchaeota was significantly lower in the BLNR group compared to ALNR ($p < 0.05$) (Figure 5C).

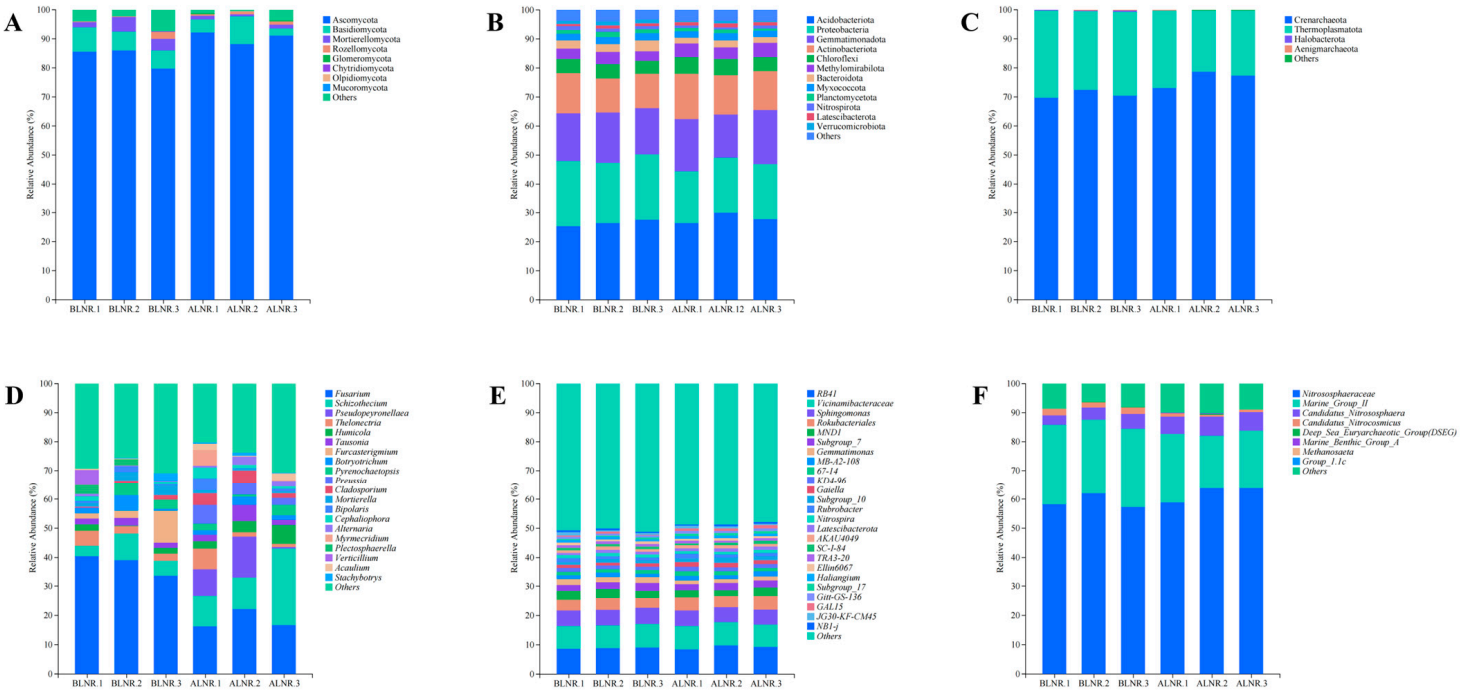

Figure 5. Effects of the low-temperature period on soil microorganism ((**A**): fungi phylum level; (**B**): bacteria phylum level; (**C**): archaea phylum level; (**D**): fungi genus level; (**E**): bacteria genus level; (**F**): archaea genus level).

Before and after the low-temperature period, fungal community composition at the genus level differed significantly between group BLNR and group ALNR ($p < 0.05$). Independent sample *t*-tests revealed a significantly higher relative abundance of Fusarium in group BLNR (37.67%) compared to group ALNR (18.47%). *Preussia* was markedly enriched in group ALNR (4.25%) relative to group BLNR (0.11%). The magnitude of these differences was substantial, with an absolute abundance increase of 19.20% for Fusarium in group BLNR and 4.14% for Preussia in group ALNR. (Figure 5D). Comparative analysis of the relative abundance of bacterial taxa at the genus level revealed significant differences, with seven exhibiting statistically significant disparities ($p < 0.05$) between group BLNR and group ALNR. The relative abundance of *Sphingomonas* was significantly higher in BLNR (5.34%) compared to ALNR (5.09%). Gemmatimonas demonstrated a markedly greater abundance in BLNR (2.07%) than in group ALNR (1.27%). Conversely, the abundance of Gaiella was higher in group ALNR (1.51%) than in BLNR (1.04%). Subgroup_17 was nearly twice as abundant in group ALNR (0.95%) compared to BLNR (0.56%). Furthermore, the abundances of Gitt-GS-136 and GAL15 were also significantly greater in group ALNR (Figure 5E). In archaea, the BLNR group exhibited significantly higher abundances of Marine_group_II and Candidatus_Nitrocosmicus compared to the ALNR group, while Candidatus_Nitrososphaera was significantly lower than in the ALNR (Figure 5F).

Temperature is a critical factor influencing microbial activity. This study evaluated the impact of the cold season on soil microbial composition by comparing biodiversity data from before and after this period. Research indicates that low temperatures significantly reduce microbial metabolism, decrease enzyme activity, increase the accumulation of recalcitrant organic matter in soil, and enhance parasitic microorganisms, with slow nutrient cycling in the soil [63]. For instance, as measured by the ^{3}H-leucine incorporation method, the bacterial growth rate at 4 °C was only one-tenth of that observed at 35 °C [64]. Similarly to the results of this experiment, the phylum-level abundances of Ascomycota, *Proteobacteria*, and *Verrucomicrobiota* in the soil were significantly lower after the cold period than before it, whereas *Crenarchaeota* showed the opposite trend (Figure 5A–C). At the genus level, similar patterns emerged: *Fusarium*, *Sphingomonas*, *Gemmatimonas*, *Marine_Group_II*, and *Candidatus_Nitrocosmicus* exhibited significant abundance declines following the cold period (Figure 5D–F). The literature has demonstrated that as temperatures decrease, the growth rates and metabolic enzyme activities of certain cold-tolerant or psychrophilic microorganisms begin to increase [63,65]. Following the onset of freeze–thaw cycles during the cold season, as soil temperatures gradually rise, thermophilic bacteria begin to revive and decompose complex organic matter, providing decomposition products for other microorganisms. Some bacteria undergo lysis and die, while psychrophilic bacteria further metabolize necrotic material, thereby promoting soil nutrient cycling [63,66]. In this study, the abundance of *Preussia*, *Gaiella*, *Subgroup_17*, *Gitt-GS-136*, *GAL15*, and *Candida-tus_Nitrososphaera* increased as temperature decreased (Figure 5D–F).

The changes in soil microbial community composition under different treatment conditions after the low-temperature period are shown in Figure 6. At the fungi phylum level, analysis using independent sample t-tests revealed significant differences in the relative abundance of Rozellomycota and Mucoromycota between ALNR and ALSR ($p < 0.05$). With Rozellomycota, significantly higher relative abundance was observed in ALNR (0.80%) compared to group ALSR (0.01%). Mucoromycota was in a significantly higher relative abundance (0.31%) in ALSR compared to ALNR (0.03%). No statistically significant differences ($p > 0.05$) were detected between ALNR and ALSR for the relative abundance of the remaining phyla. Notably, Mortierellomycota (1.18%) and Glomeromycota (0.25%) showed a trend towards higher abundance in ALNR (Figure 6A). As shown in Figure 6B, for bacterial phylum abundance between ALNR and ALSR, twelve of sixteen

phyla exhibited statistically significant abundance variations ($p < 0.05$). The Bacteroidota (6.44%), Proteobacteria (33%), and Firmicutes (0.5%) showed significantly higher abundance in group ALSR compared to group ALNR ($p < 0.05$). Acidobacteriota (28.14%), Gemmatimonadota (17.28%), Chloroflexi (5.38%), Methylomirabilota (4.58%), Myxococcota (0.93%), GAL15 (1.01%), and NB1-j (0.58%) demonstrated significantly higher abundance in ALNR ($p < 0.05$). No significant differences ($p > 0.05$) were detected for Actinobacteria, Planctomycota, and Verrucomicrobiota. At the archaea phylum level, Crenarchaeota and Thermoplasmatota collectively comprised > 99% of archaeal communities in both groups. Crenarchaeota abundance was 8.5% higher in ALSR (82.8%) compared to ALNR (76.3%) ($p < 0.05$); Thermoplasmatota showed an inverse pattern, with ALNR (23.5%) exhibiting higher abundance than ALSR (16.9%) ($p < 0.05$) (Figure 6C).

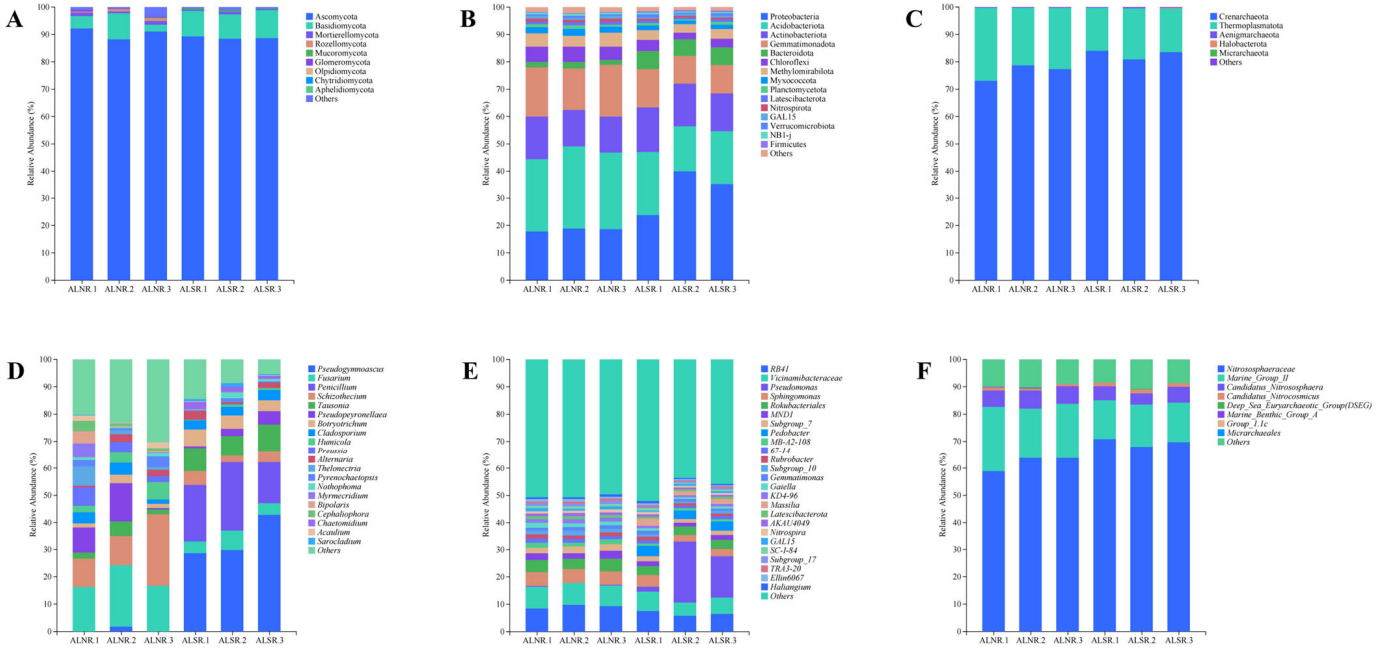

Figure 6. Effects of straw return to the field after a low-temperature period on soil microorganisms ((**A**): fungi phylum level; (**B**): bacteria phylum level; (**C**): archaea phylum level; (**D**): fungi genus level; (**E**): bacteria genus level; (**F**): archaea genus level).

At the genus level, analysis of fungal genera revealed striking compositional differences between ALNR and ALSR. Nine genera showed statistically significant abundance shifts ($p < 0.05$). In ALNR, *Fusarium* (18.47%), *Preussia* (4.25%), and *Humicola* (4.21%) were significantly higher than in ALSR, while *Pseudogymnoascus* (33.79%), *Penicillium* (20.45%), *Tausonia* (8.58%), *Botryotrichum* (5.07%), *Chaetomidium* (1.63%), and *Sarocladium* (0.96%) showed the opposite trend ($p < 0.05$) (Figure 6D). Regarding bacteria (Figure 6E), *Pedobacter* and *Massilia* were significantly higher in ALSR (3.47% and 0.01%) compared to ALNR (2.06% and 0.10%). *MND1* (2.49%), *RB41* (9.21%), *Rokubacteriales* (4.31%), *Subgroup_7* (2.30%), *MB-A2-108* (1.62%), *Gllin6067* (1.51%), *Subgroup_10* (1.43%), *KD4-96* (1.37%), *Latescibacterota* (1.05%), *GAL15* (1.01%), *AKAU4049* (1.00%), *Subgroup_17* (0.95%), and *Nitrospira* (0.92%) were significantly higher in group ALNR compared to ALSR ($p < 0.05$). As shown in the horizontal composition of Figure 6F, archaeal genus Nitrososphaeraceae and *Candidatus_Nitrocosmicus* were significantly higher in ALSR (69.43% and 1.49%) compared to ALNR (62.13% and 1.01%). *Marine_Group_II* was significantly higher in ALNR (20.65%) compared to ALSR (14.93%) ($p < 0.05$).

Microorganisms are the primary drivers of biogeochemical transformations in soil, facilitating cycling through the secretion of extracellular enzymes and the uptake of metabo-

lites. A diverse array of microbial taxa directly contribute to the degradation of organic matters. For example, the fungal genus *Penicillium* has fast growth, can secrete a variety of lignocellulose-degrading enzymes, including hemicellulases, cellulases, lignin peroxidases, manganese peroxidases, and laccases, and can exhibit strong lignocellulose degradation, breaking down crop residue roots and stems [67,68]. At a broader taxonomic level, key microbial phyla also play specialized roles in this process. *Mucoromycota* fungi act as foundational decomposers, maintaining basal enzyme activity even at low temperatures and producing metabolites that support the wider microbial community [69,70]. Among bacteria, Bacteroidetes, Proteobacteria, and Firmicutes are the primary agents of soil carbon metabolism, exhibiting greater specificity in the decomposition of lignocellulose [71–74]. Other strains, however, exhibit lower relative abundances during growth. This is because they rely on simple or specific carbon sources (such as humic substances or one-carbon compounds), adapt to oligotrophic environments, or experience suppressed metabolic activity at low temperatures, making them unable to compete effectively against "straw-degrading specialized bacteria [75,76]. After the low-temperature period with straw return treatment, the relative abundance of *Mucoromycota*, *Bacteroidota*, *Proteobacteria*, *Firmicutes*, and *Crenarchaeota* showed significant positive differences, while *Rozellomycota*, *Acidobacteriota*, *Gemmatimonadota*, *Chloroflexi*, *Methylomirabilota*, *Myxococcota*, GAL15, NB1-j, and *Thermoplasmatota* showed the opposite trend (Figure 6A–C). At the genus level, the results of this experiment indicate that *Pseudogymnoascus*, *Penicillium*, *Tausonia*, *Botryotrichum*, *Chaetomidium*, *Sarocladium*, *Pedobacter*, *Massilia*, *Nitrososphaeraceae*, and *Candidatus_Nitrocosmicus* significantly increased in the soil of the straw-returning treatment group after the low-temperature period (Figure 6D–F). *Botryotrichum* is able to produce cellulases and other lignocellulosic-degrading enzymes [77]. Some studies have shown that *Botryotrichum* is tolerant to high temperatures and arid environments [78]; *Pseudogymnoascus* is a class of cryophilic fungi, widely distributed in the cold regions of the earth [79], and some studies have shown that *Pseudogymnoascus* has good enzyme-producing activity in low-temperature environments and can promote lignocellulose degradation [80]; *Pseudomonas* has a high degree of functional diversity and adaptability, which enables it to effectively depolymerize lignocellulosic biomass [81], and *Pseudomonas* can effectively degrade lignocellulose and accelerate lignocellulosic biotransformation when it combines with other bacteria to form bacterial cons *Pseudogymnosousortia*, e.g., *P. mosselii* SSA-1568 with *Shewanella sp. SSA-1557* and *Bacillus cereus SSA-1558* [82]. *Pedobacter* is widely present in soil and can produce various degrading enzymes, including cellulase, hemicellulase, and pectinase [83], among which *Pedobacter sp. PAMC26386* has strong cold tolerance [84]. In cold regions with low temperatures, the focus of straw-degrading microorganisms should be on cold-tolerant or cold-loving microorganisms, such as the dominant fungi *Pseudogymnoascus*, *Penicillium*, and *Botryotrichum*, which can degrade straw under low-temperature freezing and thawing environments, and the dominant bacteria in this study, *Pseudomonas* and *Pedobacter*, which cleave straw into various nutrients which are subsequently released into the soil, contributing to the improvement of soil physical properties. (Figures 5 and 6, RDA analysis of microorganisms and environmental factors is provided in Appendix A).

4. Conclusions

This study demonstrates that the winter period in cold regions, characterized by freeze–thaw cycles, plays a critical role in the initial physical breakdown of maize straw. This process accounted for approximately one-quarter of the first year's total decomposition in the saline alkali farmland examined. Although the freezing conditions suppressed overall microbial activity and reduced the availability of soil nutrients, the practice of straw returning effectively mitigated these adverse effects. The incorporated straw improved

soil structure, porosity, water retention, and nutrient availability More importantly, the straw amendment shaped a distinct microbial community enriched with cold-tolerant taxa such as *Pseudogymnoascus*, *Penicillium*, and *Pedobacter*. These taxa possess lignocellulolytic capabilities, making them pivotal for initiating straw decomposition under low-temperature stress. Therefore, straw returning not only enhances soil quality and resistance to winter erosion but also cultivates a functional microbial consortium, thereby promoting sustainable agroecosystem management in cold, saline-alkali regions.

Author Contributions: Conceptualization, W.W. and W.Z.; data curation, W.Z.; formal analysis, W.Z.; funding acquisition, W.W. and G.S.; investigation, W.Z. and J.W.; methodology, W.W. and W.Z.; project administration, G.S.; resources, W.W. and G.S.; software, D.W. and W.W.; supervision, D.W. and W.W.; validation, W.Z. and J.W.; visualization, W.Z. and A.K.; writing—original draft preparation, W.Z.; writing—review and editing, W.Z. and A.K. All authors have read and agreed to the published version of the manuscript.

Funding: This research was funded by National Key Research Program and Development plan (2023YFD1500501), Heilongjiang Science and Technology Project (2022ZX108B01), the Fundamental Research Funds for the Central Universities (2572023CT08), National Natural Science Foundation of China, (U22A20444), National Key Research Program and Development plan (2025YFD1700201).

Data Availability Statement: The original contributions presented in this study are included in the article. Further inquiries can be directed to the corresponding authors.

Acknowledgments: We extend our gratitude to the College of Agriculture at Heilongjiang Bayi Agricultural University for providing the experimental site. During the preparation of this manuscript, the author used DeepSeek-V3 to fix grammatical errors. Thanks to DeepSeek for the help. The authors have reviewed and edited the output and take full responsibility for the content of this publication.

Conflicts of Interest: The authors declare that there are no conflicts of interest.

Abbreviations

The following abbreviations are used in this manuscript:

BLNR	Before the low temperature period (BL) and non-straw return treatment (NR)
ALNR	After the low temperature period (AL) and non-straw return treatment (NR)
ALSR	After the low temperature period (AL) and the straw return treatment (SR)

Appendix A

Analysis of Figures A1 and A2 reveals that while both axes of the RDA analysis demonstrate good explanatory power, significant correlations between bacteria and soil physical properties were only observed in the straw-returning treatment group. No other significant differences emerged. The coordinate quadrants indicate that soil quality was generally favorable prior to the low-temperature period, with the straw-returning treatment group showing a positive trend in both soil nutrients and quality.

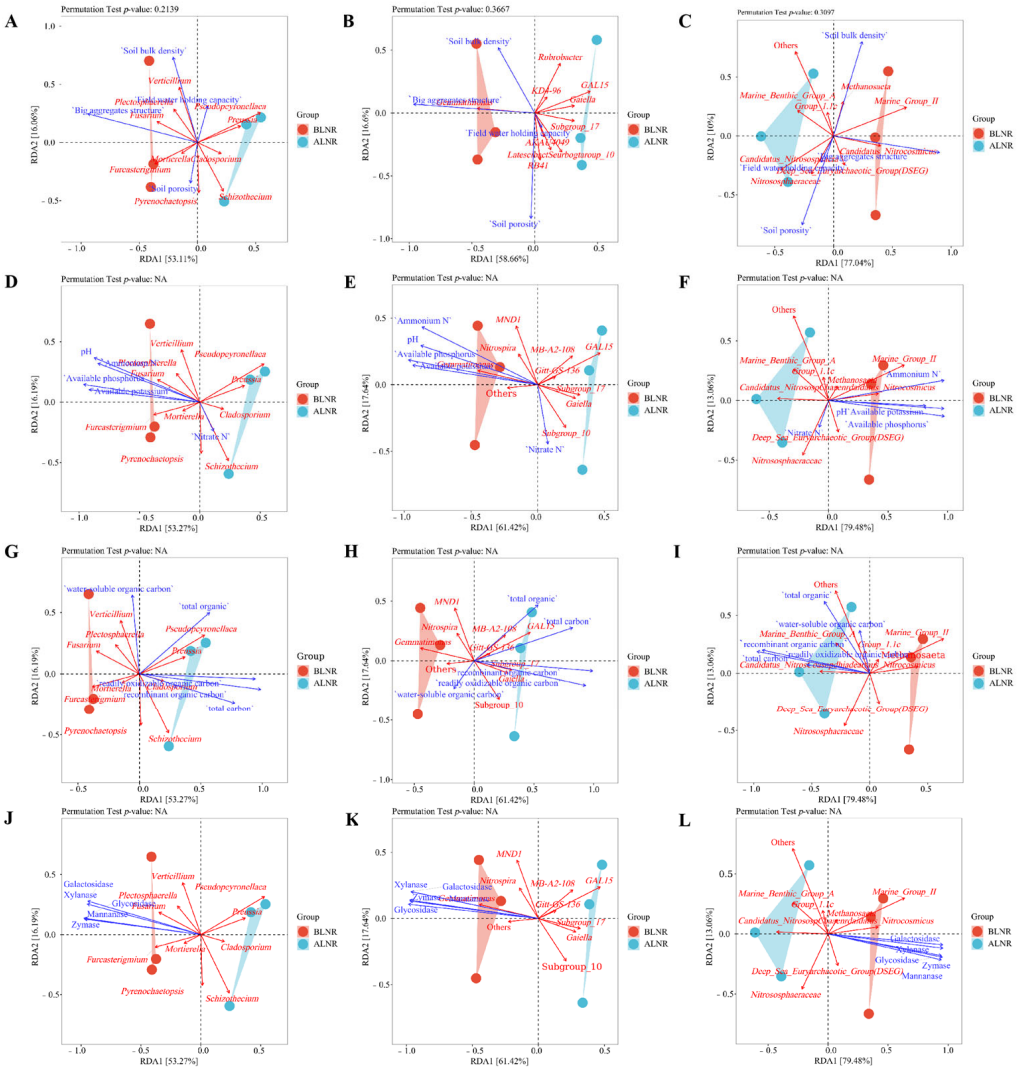

Figure A1. RDA **analysis of soil microorganisms and soil environmental factors (soil physicochemical properties, soil carbon content, and straw degradation enzyme activity) before and after the low-temperature period** ((**A**): fungi–physico; (**B**): bacteria–physico; (**C**): archaea–physico; (**D**): fungi–chemical; (**E**): bacteria–chemical; (**F**): archaea–chemical; (**G**): fungi–carbon content; (**H**): bacteria–carbon content; (**I**): archaea–carbon content; (**J**): fungi–straw degradation enzyme activity; (**K**): bacteria–straw degradation enzyme activity; (**L**): archaea–straw degradation enzyme activity).

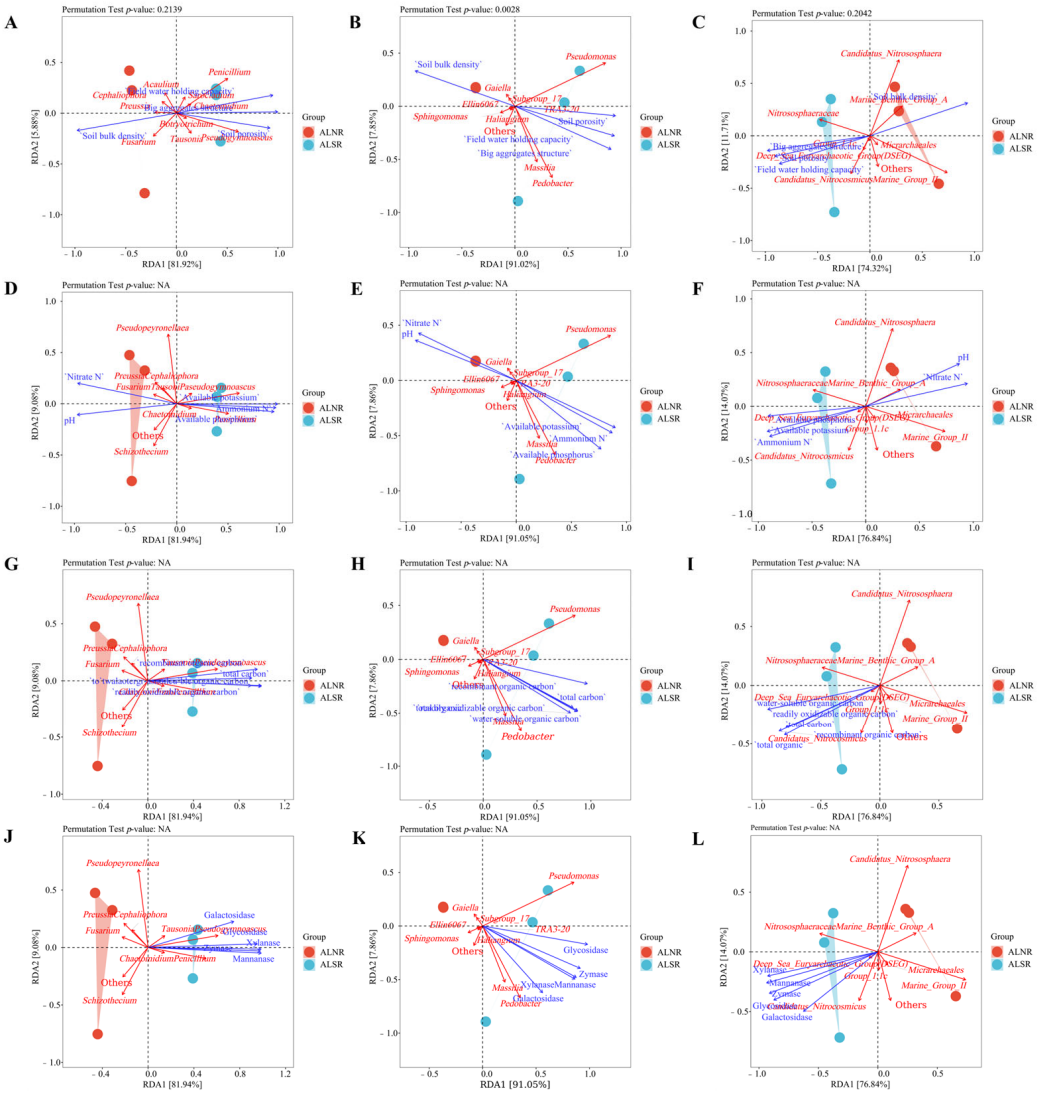

Figure A2. RDA analysis of soil microorganisms and soil environmental factors (soil physicochemical properties, soil carbon content, straw degradation enzyme activity) under straw-returning and non-returning treatments after the low-temperature period ((**A**): fungi–physico; (**B**): bacteria–physico; (**C**): archaea–physico; (**D**): fungi–chemical; (**E**): bacteria–chemical; (**F**): archaea–chemical; (**G**): fungi–carbon content; (**H**): bacteria–carbon content; (**I**): archaea–carbon content; (**J**): fungi–straw degradation enzyme activity; (**K**): bacteria–straw degradation enzyme activity; (**L**): archaea–straw degradation enzyme activity)).

References

1. Chen, L.; Sun, S.; Yao, B.; Peng, Y.; Gao, C.; Qin, T.; Zhou, Y.; Sun, C.; Quan, W. Effects of straw return and straw biochar on soil properties and crop growth: A review. *Front. Plant Sci.* **2022**, *13*, 986763. [CrossRef] [PubMed]
2. Yang, L.; Muhammad, I.; Chi, Y.X.; Liu, Y.X.; Wang, G.Y.; Wang, Y.; Zhou, X.B. Straw return and nitrogen fertilization regulate soil greenhouse gas emissions and global warming potential in dual maize cropping system. *Sci. Total. Environ.* **2022**, *853*, 158370. [CrossRef]
3. Wahdan, S.F.M.; Ji, L.; Schädler, M.; Wu, Y.-T.; Sansupa, C.; Tanunchai, B.; Buscot, F.; Purahong, W. Future climate conditions accelerate wheat straw decomposition alongside altered microbial community composition, assembly patterns, and interaction networks. *ISME J.* **2023**, *17*, 238–251. [CrossRef] [PubMed]
4. Wang, Y.; Li, F.Y.; Song, X.; Wang, X.; Suri, G.; Baoyin, T. Changes in Litter Decomposition Rate of Dominant Plants in a Semi-Arid Steppe Across Different Land-Use Types: Soil Moisture, Not Home-Field Advantage, Plays a Dominant Role. *Agric. Ecosyst. Environ.* **2020**, *303*, 107119. [CrossRef]

5. Portela, S.I.; Reixachs, C.; Torti, M.J.; Beribe, M.J.; Giannini, A.P. Contrasting Effects of Soil Type and Use of Cover Crops on Nitrogen and Phosphorus Leaching in Agricultural Systems of the Argentinean Pampas. *Agric. Ecosyst. Environ.* **2024**, *364*, 108897. [CrossRef]
6. Merino-Martín, L.; Stokes, A.; Gweon, H.S.; Moragues-Saitua, L.; Staunton, S.; Plassard, C.; Oliver, A.; Bissonnais, Y.L.; Griffiths, R.I. Interacting effects of land use type, soil microbes and plant traits on aggregate stability. *Soil Biol. Biochem.* **2021**, *154*, 108072. [CrossRef]
7. Eduah, J.O.; Nartey, E.K.; Abekoe, M.K.; Breuning-Madsen, H.; Andersen, M.N. Phosphorus retention and availability in three contrasting soils amended with rice husk and corn cob biochar at varying pyrolysis temperatures. *Geoderma* **2019**, *341*, 10–17. [CrossRef]
8. Wang, J.; Xu, C.; Zhang, W.; Hong, Y.; Shen, G.; Wang, W.; Tang, H.; Zhang, S.; Pan, J.; Wang, W. Synergistic effect of two bacterial strains promoting anaerobic digestion of rice straw to produce methane. *Environ. Res.* **2024**, *252*, 118974. [CrossRef]
9. Wang, K.; Hu, W.; Xu, Z.; Xue, Y.; Zhang, Z.; Liao, S.; Zhang, Y.; Li, X.; Ren, T.; Cong, R.; et al. Seasonal Temporal Characteristics of In Situ Straw Decomposition in Different Types and Returning Methods. *J. Soil Sci. Plant Nut.* **2022**, *22*, 4228–4240. [CrossRef]
10. Nguyen, J.; Lara-Gutiérrez, J.; Stocker, R. Environmental fluctuations and their effects on microbial communities, populations and individuals. *Fems. Microbiol. Rev.* **2021**, *45*, fuaa068. [CrossRef]
11. Wang, X.; Lu, J.; Zhang, X.; Wang, P. Contrasting microbial mechanisms of soil priming effects induced by crop residues depend on nitrogen availability and temperature. *Appl. Soil Ecol.* **2021**, *168*, 104186. [CrossRef]
12. Huang, F.; Ding, X.; Li, W.; Jia, H.; Wei, X.; Zhao, X. The effect of temperature on the decomposition of different parts of maize residues in a solonchak. *Catena* **2021**, *201*, 105207. [CrossRef]
13. Sun, B.; Wang, X.; Wang, F.; Jiang, Y.; Zhang, X.-X. Assessing the Relative Effects of Geographic Location and Soil Type on Microbial Communities Associated with Straw Decomposition. *Appl. Environ. Microb.* **2013**, *79*, 3327–3335. [CrossRef] [PubMed]
14. Xie, S.; Dou, S.; Fu, J.; Ma, R. Corn straw return effectively improves the stability and increases the carbon and nitrogen contents of waterstable aggregates in northeastern China black soil. *Bragantia* **2023**, *82*, e20220218. [CrossRef]
15. Nabi, F.; Chen, H.; Sajid, S.; Yang, G.; Kyung, Y.; Shah, S.M.M.; Wang, X.; Hu, Y. Degradation of agricultural waste is dependent on chemical fertilizers in long-term paddy-dry rotation field.15. *J. Environ. Manag.* **2024**, *355*, 120460. [CrossRef]
16. Şahin, Y.; Akkaya, Y.; Taşdemir, M.A. Effects of freezing conditions on the frost resistance and microstructure of concrete. *Constr. Build. Mater.* **2021**, *270*, 121458. [CrossRef]
17. Jia, G.; Chen, Y.; Sun, A.; Orlien, V. Control of ice crystal nucleation and growth during the food freezing process. *Compr. Rev. Food Sci. Food Saf.* **2022**, *21*, 2433–2454. [CrossRef]
18. Raza, T.; Qadir, M.F.; Khan, K.S.; Eash, N.S.; Yousuf, M.; Chatterjee, S.; Manzoor, R.; Rehman, S.U.; Oetting, J.N. Unraveling the potential of microbes in decomposition of organic matter and release of carbon in the ecosystem. *J. Environ. Manag.* **2023**, *344*, 118529. [CrossRef]
19. Cruz-Paredes, C.; Tájmel, D.; Rousk, J. Can moisture affect temperature dependences of microbial growth and respiration? *Soil Biol. Biochem.* **2021**, *156*, 108223. [CrossRef]
20. Xu, H.; Huang, L.; Chen, J.; Zhou, H.; Wan, Y.; Qu, Q.; Wang, M.; Xue, S. Changes in Soil Microbial Activity and Their Linkages with Soil Carbon under Global Warming. *Catena* **2023**, *232*, 107419. [CrossRef]
21. Mu, X.; Zhang, S.; Lv, X.; Ma, Y.; Zhang, Z.; Han, B. Water flow and temperature drove epiphytic microbial community shift: Insight into nutrient removal in constructed wetlands from microbial assemblage and co-occurrence patterns. *Bioresour. Technol.* **2021**, *332*, 125134. [CrossRef]
22. Li, S.; Cui, Y.; Xia, Z.; Zhang, X.; Zhou, C.; An, S.; Zhu, M.; Gao, Y.; Yu, W.; Ma, Q. Microbial nutrient limitations limit carbon sequestration but promote nitrogen and phosphorus cycling: A case study in an agroecosystem with long-term straw return. *Sci. Total Environ.* **2023**, *870*, 161865. [CrossRef]
23. Gebremedhin, M.T.; Loescher, H.W.; Tsegaye, T.D. Carbon Balance of No-Till Soybean with Winter Wheat Cover Crop in the Southeastern United States. *Agron. J.* **2012**, *104*, 1321–1335. [CrossRef]
24. Song, C.; Dai, C.; Wang, C.; Yu, M.; Gao, Y.; Tu, W. Characteristic Analysis of the Spatio-Temporal Distribution of Key Variables of the Soil Freeze–Thaw Processes over Heilongjiang Province, China. *Water* **2022**, *14*, 2573. [CrossRef]
25. Wang, X.; Li, Y.; Zhang, L.; Song, S.; Pan, T.; Ren, C.; Tan, Y. Mechanism and effects of the increase in winter temperatures in the Arctic region on cold winters in Heilongjiang Province, Northeast China for the period 1961–2018. *J. Geogr. Sci.* **2022**, *32*, 225–240. [CrossRef]
26. Wang, X.; Wang, X.; Geng, P.; Yang, Q.; Chen, K.; Liu, N.; Fan, Y.; Zhan, X.; Han, X. Effects of different returning method combined with decomposer on decomposition of organic components of straw and soil fertility. *Sci. Rep.* **2021**, *11*, 15495. [CrossRef]
27. Hopmans, J.W.; Qureshi, A.S.; Kisekka, I.; Munns, R.; Grattan, S.R.; Rengasamy, P.; Ben-Gal, A.; Assouline, S.; Javaux, M.; Minhas, P.S.; et al. Critical knowledge gaps and research priorities in global soil salinity. *Adv. Agron.* **2021**, *169*, 1–191. [CrossRef]
28. Hou, R.-J.; Li, T.-X.; Fu, Q.; Liu, D.; Li, M.; Zhou, Z.-Q.; Yan, J.-W.; Zhang, S. Research on the Distribution of Soil Water, Heat, Salt and Their Response Mechanisms under Freezing Conditions. *Soil Till. Res.* **2020**, *196*, 104486. [CrossRef]

29. Ginot, F.; Lenavetier, T.; Dedovets, D.; Deville, S. Solute Strongly Impacts Freezing under Confinement. *Appl. Phys. Lett.* **2020**, *116*, 253701. [CrossRef]
30. Chengyou, C.; Shuang, T.; Zhenbo, C.; Ying, Z. Response of Soil Properties and Microbial Communities to Increasing Salinization in the Meadow Grassland of Northeast China. *Microb. Ecol.* **2021**, *82*, 722–735. [CrossRef] [PubMed]
31. Chase, J.M. Drought Mediates the Importance of Stochastic Community Assembly. *Proc. Natl. Acad. Sci. USA* **2007**, *104*, 17430–17434. [CrossRef]
32. Li, Y.; Cha, Q.-Q.; Dang, Y.-R.; Chen, X.-L.; Wang, M.; McMinn, A.; Espina, G.; Zhang, Y.-Z.; Blamey, J.M.; Qin, Q.-L. Reconstruction of the Functional Ecosystem in the High Light, Low Temperature Union Glacier Region, Antarctica. *Front. Cell. Infect. Microbiol.* **2019**, *10*, 02408. [CrossRef] [PubMed]
33. Bradley, J.A.; Trivedi, C.B.; Winkel, M.; Mourot, R.; Lutz, S.; Larose, C.; Keuschnig, C.; Doting, E.; Halbach, L.; Zervas, A.; et al. Active and dormant microorganisms on glacier surfaces. *Geobiology* **2022**, *21*, 244–261. [CrossRef]
34. Wei, S.; Liu, K.; Ji, X.; Wang, T.; Wang, R. Application of enzyme technology in biopulping and biobleaching. *Cellulose* **2021**, *28*, 10099–10116. [CrossRef]
35. Hamid, B.; Bashir, Z.; Yatoo, A.M.; Mohiddin, F.; Majeed, N.; Bansal, M.; Poczai, P.; Almalki, W.H.; Sayyed, R.Z.; Shati, A.A.; et al. Cold-Active Enzymes and Their Potential Industrial Applications—A Review. *Molecules* **2022**, *27*, 5885. [CrossRef] [PubMed]
36. Zhang, G.S.; Liu, Y.F. The distribution of microplastics in soil aggregate fractions in southwestern China. *Sci. Total Environ.* **2018**, *642*, 12–20. [CrossRef]
37. Zhang, G.S.; Hu, X.B.; Zhang, X.X.; Li, J. Effects of plastic mulch and crop rotation on soil physical properties in rain-fed vegetable production in the mid-Yunnan plateau, China. *Soil Till. Res.* **2015**, *145*, 111–117. [CrossRef]
38. Ruirui, C.; Xiaoting, W. *BOOK REVIEW: Analytical Methods for Soil and Agro-Chemistry*; Zhu, H.Z., He, P.A., Chen, C.Z., Zhou, H.M., Su, D.C., Xu, J.M., Qin, H.Y., Bao, S.D., Lu, S.R.K., Jiang, H., Eds.; Soil Science Society of China; Agricultural Science and Technology Press: Beijing, China, 2000; p. 638. ISBN 9787801199256. (In Chinese) [CrossRef]
39. Zhang, F.; Yu, W.; Liu, W.; Xu, Z. The Mixed Fermentation Technology of Solid Wastes of Agricultural Biomass. *Front. Energy Res.* **2020**, *8*, 00050. [CrossRef]
40. Sadalage, P.S.; Dar, M.A.; Chavan, A.R.; Pawar, K.D. Formulation of synthetic bacterial consortia and their evaluation by principal component analysis for lignocellulose rich biomass degradation. *Renew. Energy* **2020**, *148*, 467–477. [CrossRef]
41. Guan, X.-K.; Wei, L.; Turner, N.C.; Ma, S.-C.; Yang, M.-D.; Wang, T.-C. Improved straw management practices promote in situ straw decomposition and nutrient release, and increase crop production. *J. Clean. Prod.* **2020**, *250*, 119514. [CrossRef]
42. Qin, X.-C.; Meng, S.-P.; Cao, D.-F.; Tu, Y.-M.; Sabourova, N.; Grip, N.; Ohlsson, U.; Blanksvärd, T.; Sas, G.; Elfgren, L. Evaluation of freeze-thaw damage on concrete material and prestressed concrete specimens. *Constr. Build. Mater.* **2016**, *125*, 892–904. [CrossRef]
43. Zhang, K.; Zhou, J.; Yin, Z. Experimental Study on Mechanical Properties and Pore Structure Deterioration of Concrete under Freeze–Thaw Cycles. *Materials* **2021**, *14*, 6568. [CrossRef] [PubMed]
44. Wang, S.; Qin, J.; Zheng, K.; Yang, F.; Zhang, Y.; Wei, S.; Ren, D. Study on Physical Properties and Energy Evolution of Natural Gypsum Rock under Freeze-thaw Cycles. *Int. J. Energy Res.* **2023**, *2*, 72–75. [CrossRef]
45. Zhang, J.; Deng, H.; Taheri, A.; Ke, B.; Liu, C.; Yang, X. Degradation of physical and mechanical properties of sandstone subjected to freeze-thaw cycles and chemical erosion. *Cold Reg. Sci. Technol.* **2018**, *155*, 37–46. [CrossRef]
46. Luo, X.; Zhou, S.; Huang, B.; Jiang, N.; Xiong, M. Effect of Freeze–Thaw Temperature and Number of Cycles on the Physical and Mechanical Properties of Marble. *Geotech. Geol. Eng.* **2020**, *39*, 567–582. [CrossRef]
47. Zhang, S.; Wang, X.; Xiao, Z.; Qu, F.; Wang, X.; Li, Y.; Aurangzeib, M.; Zhang, X.; Liu, X. Quantitative Studies of Gully Slope Erosion and Soil Physiochemical Properties During Freeze-Thaw Cycling in a Mollisol Region. *Sci. Total Environ.* **2019**, *707*, 136191. [CrossRef]
48. Liu, S.; Huang, Q.; Zhang, W.; Ren, D.; Xu, X.; Xiong, Y.; Huang, G. An Improved Estimation of Soil Water and Salt Dynamics by Considering Soil Bulk Density Changes under Freeze/thaw Conditions in Arid Areas with Shallow Groundwater Tables. *Sci. Total Environ.* **2023**, *859*, 160342. [CrossRef]
49. Liu, B.; Fan, H.; Han, W.; Zhu, L.; Zhao, X.; Zhang, Y.; Ma, R. Linking soil water retention capacity to pore structure characteristics based on X-ray computed tomography: Chinese Mollisol under freeze-thaw effect. *Geoderma* **2021**, *401*, 115170. [CrossRef]
50. Wang, Z.; Zhang, Y.; Flury, M.; Zou, H. Freeze-thaw Cycles Lead to Enhanced Colloid-Facilitated Pb Transport in a Chernozem Soil. *J. Contam. Hydrol.* **2022**, *251*, 104093. [CrossRef]
51. Zhai, J.; Zhang, S.; Zhang, Z.; Melnikov, A.; Li, H. Study on the geometry characteristics of soil primary mineral particles under cryogenic action. *Sci. Rep.* **2022**, *12*, 16766. [CrossRef]
52. Zhang, Y.; Fu, Y.; Xu, J.; Li, Y.; Zhao, Y.; Wei, S.; Liu, B.; Zhang, X.; Lei, H.; Shao, S. Impact of Freeze–thaw Cycling on the Stability and Turnover of Black Soil Aggregates. *Geoderma* **2024**, *449*, 117004. [CrossRef]
53. Sun, L.; Chang, X.; Yu, X.; Jia, G.; Chen, L.; Wang, Y.; Liu, Z. Effect of freeze-thaw processes on soil water transport of farmland in a semi-arid area. *Agric. Water Manag.* **2021**, *252*, 106876. [CrossRef]

54. Qiu, L.; Zhu, H.; Liu, J.; Yao, Y.; Wang, X.; Rong, G.; Zhao, X.; Shao, M.; Wei, X. Soil Erosion Significantly Reduces Organic Carbon and Nitrogen Mineralization in a Simulated Experiment. *Agric. Ecosyst. Environ.* **2021**, *307*, 107232. [CrossRef]
55. Zeng, Q.-X.; Zeng, X.-M.; Lin, K.-M.; Zhang, Q.-F.; Cheng, L.; Zhou, J.-C.; Lin, Q.-Y.; Chen, Y.-M.; Xu, J.-G. [Responses of Soil Phosphorus Fractions and Microorganisms to Nitrogen Application in a Subtropical Phyllostachys Pubescen Forest]. *J. Appl. Ecol.* **2020**, *31*, 753–760. [CrossRef]
56. Liao, J.; Dou, Y.; Yang, X.; An, S. Soil microbial community and their functional genes during grassland restoration. *Environ. Manag.* **2023**, *325*, 116488. [CrossRef]
57. Coonan, E.C.; Kirkby, C.A.; Kirkegaard, J.A.; Amidy, M.R.; Strong, C.L.; Richardson, A.E. Microorganisms and nutrient stoichiometry as mediators of soil organic matter dynamics. *Nutr. Cycl. Agroecosyst.* **2020**, *117*, 273–298. [CrossRef]
58. Huang, T.; Yang, N.; Lu, C.; Qin, X.; Siddique, K.H.M. Soil Organic Carbon, Total Nitrogen, Available Nutrients, and Yield under Different Straw return Methods. *Soil Till. Res.* **2021**, *214*, 105171. [CrossRef]
59. Huang, C.; Huang, H.; Huang, S.; Li, W.; Zhang, K.; Chen, Y.; Yang, L.; Luo, L.; Deng, L. Effects of Straw return on Soil Aggregates and Its Organic Carbon and Nitrogen Retention under Different Mechanized Tillage Modes in Typical Hilly Regions of Southwest China. *Agronomy* **2024**, *14*, 928. [CrossRef]
60. Song, J.; Huang, J.; Gao, J.-S.; Wang, Y.-N.; Wu, C.-X.; Bai, L.-Y.; Zeng, X.-B. Effects of Green Manure Planted in Winter and Straw return on Soil Aggregates and Organic Matter Functional Groups in Double Cropping Rice Area. *J. Appl. Ecol.* **2021**, *32*, 564–570. [CrossRef]
61. Bai, T.; Ran, C.; Ma, Q.; Miao, Y.; Li, S.; Lan, H.; Li, X.; Chen, Q.; Zhang, Q.; Shao, X. The Application of Straw Return with Nitrogen Fertilizer Increases Rice Yield in Saline–Sodic Soils by Regulating Rice Organ Ion Concentrations and Soil Leaching Parameters. *Agronomy* **2024**, *14*, 2807. [CrossRef]
62. Curtright, A.J.; Tiemann, L.K. Intercropping Increases Soil Extracellular Enzyme Activity: A Meta-Analysis. *Agric. Ecosyst. Environ.* **2021**, *319*, 107489. [CrossRef]
63. Donhauser, J.; Qi, W.; Bergk-Pinto, B.; Frey, B. High Temperatures Enhance the Microbial Genetic Potential to Recycle C and N from Necromass in High-mountain Soils. *Glob. Change Biol.* **2020**, *27*, 1365–1386. [CrossRef]
64. Donhauser, J.; Niklaus, P.A.; Rousk, J.; Larose, C.; Frey, B. Temperatures Beyond the Community Optimum Promote the Dominance of Heat-Adapted, Fast Growing and Stress Resistant Bacteria in Alpine Soils. *Soil Biol. Biochem.* **2020**, *148*, 107873. [CrossRef]
65. Misiak, M.; Goodall-Copestake, W.P.; Sparks, T.H.; Worland, M.R.; Boddy, L.; Magan, N.; Convey, P.; Hopkins, D.W.; Newsham, K.K. Inhibitory Effects of Climate Change on the Growth and Extracellular Enzyme Activities of a Widespread Antarctic Soil Fungus. *Glob. Change Biol.* **2020**, *27*, 1111–1125. [CrossRef] [PubMed]
66. Dahl, M.B.; Kreyling, J.; Petters, S.; Wang, H.; Mortensen, M.S.; Maccario, L.; Sorensen, S.J.; Urich, T.; Weigel, R. Warmer Winters Result in Reshaping of the European Beech Forest Soil Microbiome (bacteria, Archaea and Fungi)—With Potential Implications for Ecosystem Functioning. *Environ. Microbiol.* **2023**, *25*, 1118–1135. [CrossRef]
67. Guo, Y.; Zhang, Z.; Dou, J.; Liu, G.; Li, X.; Zhao, J. Structural Characterization of Corn Fiber Hemicelluloses Extracted by Organic Solvent and Screening of Degradation Enzymes. *Int. J. Antimicrob. Agents* **2023**, *313*, 120820. [CrossRef]
68. Jia, H.; Feng, X.; Huang, J.; Guo, Y.; Zhang, D.; Li, X.; Zhao, J. Recombinant Family 1 Carbohydrate-Binding Modules Derived from Fungal Cellulase Enhance Enzymatic Degradation of Lignocellulose as Novel Effective Accessory Protein. *Front. Microbiol.* **2022**, *13*, 876466. [CrossRef]
69. Sepideh, P.; Nurulfarhana, H.; Shahir, S.M.; Jafar, R. Psychrophilic Enzymes: Structural Adaptation, Pharmaceutical and Industrial Applications. *Appl. Microbiol. Biot.* **2021**, *105*, 899–907. [CrossRef]
70. Dzurendova, S.; Losada, C.B.; Dupuy-Galet, B.X.; Fjær, K.; Shapaval, V. Mucoromycota Fungi as Powerful Cell Factories for Modern Biorefinery. *Appl. Microbiol. Biot.* **2021**, *106*, 101–115. [CrossRef]
71. López-Mondéjar, R.; Algora, C.; Baldrian, P. Lignocellulolytic systems of soil bacteria: A vast and diverse toolbox for biotechnological conversion processes. *Biotechnol. Adv.* **2019**, *37*, 107374. [CrossRef] [PubMed]
72. Gavande, P.V.; Basak, A.; Sen, S.; Lepcha, K.; Murmu, N.; Rai, V.; Mazumdar, D.; Saha, S.P.; Das, V.; Ghosh, S. Functional Characterization of Thermotolerant Microbial Consortium for Lignocellulolytic Enzymes with Central Role of Firmicutes in Rice Straw Depolymerization. *Sci. Rep.* **2021**, *11*, 3032. [CrossRef]
73. Kim, S.-R.; Lee, J.; Lee, M.G.; Sung, H.G.; Hwang, S.-G. Analysis of Microbial Communities in Solid and Liquid Pig Manure During the Fertilization Process. *Sci. Rep.* **2024**, *14*, 72. [CrossRef] [PubMed]
74. Geng, A.; Jin, M.; Li, N.; Zhu, D.; Xie, R.; Wang, Q.; Lin, H.; Sun, J. New Insights into the Co-Occurrences of Glycoside Hydrolase Genes among Prokaryotic Genomes Through Network Analysis. *Microorganisms* **2021**, *9*, 427. [CrossRef]
75. Soong, J.L.; Fuchslueger, L.; Maranon-Jimenez, S.; Torn, M.S.; Janssens, I.A.; Penuelas, J.; Richter, A. Microbial Carbon Limitation: The Need for Integrating Microorganisms into Our Understanding of Ecosystem Carbon Cycling. *Glob. Change Biol.* **2020**, *26*, 1953–1961. [CrossRef]

76. Mcnichol, S.M.; Sanchez-Quete, F.; Loeb, S.K.; Teske, A.P.; Walter, S.R.S.; Mahmoudi, N. Dynamics of Carbon Substrate Competition among Heterotrophic Microorganisms. *ISME J.* **2024**, *18*, wrae018. [CrossRef]
77. Andlar, M.; Rezić, T.; Marđetko, N.; Kracher, D.; Ludwig, R.; Šantek, B. Lignocellulose degradation: An overview of fungi and fungal enzymes involved in lignocellulose degradation. *Eng. Life Sci.* **2018**, *18*, 768–778. [CrossRef] [PubMed]
78. Ebrahim, W.; Ebada, S.S. Antimicrobial Metabolites from Extremophilic Fungus *Botryotrichum piluliferum* Strain WESH19. *Chem. Nat. Compd.* **2021**, *57*, 654–658. [CrossRef]
79. Kim, Y.-S.; Lee, S.-Y.; Chung, C.-U.; Park, J.-S.; Kim, Y.-J.; Oem, J.-K. Fungal Diversity in Korean Caves and Cave-Inhabiting Bats with Attention to Pseudogymnoascus Species. *Diversity* **2023**, *15*, 198. [CrossRef]
80. Yoshinaga, T.T.; Giovanella, P.; de Farias, G.S.; dos Santos, J.A.; Pellizzer, E.P.; Sette, L.D. Fungi from Antarctic Marine Sediment: Characterization and Assessment for Textile Dye Decolorization and Detoxification. *Braz. J. Microbiol.* **2024**, *55*, 3437–3448. [CrossRef] [PubMed]
81. Georgiadou, D.N.; Avramidis, P.; Ioannou, E.; Hatzinikolaou, D.G. Microbial Bioprospecting for Lignocellulose Degradation at a Unique Greek Environment. *Heliyon* **2020**, *7*, e07122. [CrossRef]
82. Ali, S.S.; Jiao, H.; El-Sapagh, S.; Sun, J. Biodegradation of Willow Sawdust by Novel Cellulase-Producing Bacterial Consortium from Wood-Feeding Termites for Enhancing Methane Production. *Bioresour. Technol.* **2023**, *383*, 129232. [CrossRef] [PubMed]
83. Miao, Q.; Zhang, X.; Wang, Y.; Li, X.; Wang, Z.; Tian, L.; Qu, L.; Wei, Y. Characterization of Novel Pectinolytic Enzymes Derived from the Efficient Lignocellulose Degradation Microbiota. *Biomolecules* **2022**, *12*, 1388. [CrossRef] [PubMed]
84. Cho, C.-Y.; Han, S.-R.; Oh, T.-J. Complete Genome Sequence of *Pedobacter* sp. PAMC26386 and Their Low Temperature Application in Arabinose-containing Polysaccharides Degradation. *Curr. Microbiol.* **2021**, *78*, 944–953. [CrossRef] [PubMed]

Disclaimer/Publisher's Note: The statements, opinions and data contained in all publications are solely those of the individual author(s) and contributor(s) and not of MDPI and/or the editor(s). MDPI and/or the editor(s) disclaim responsibility for any injury to people or property resulting from any ideas, methods, instructions or products referred to in the content.